We are IntechOpen, the world's leading publisher of Open Access books Built by scientists, for scientists

4,800
Open access books available

122,000
International authors and editors

135M
Downloads

Our authors are among the

154
Countries delivered to

TOP 1%
most cited scientists

12.2%
Contributors from top 500 universities

CLARIVATE ANALYTICS BOOK CITATION INDEX INDEXED

WEB OF SCIENCE™

Selection of our books indexed in the Book Citation Index in Web of Science™ Core Collection (BKCI)

Interested in publishing with us?
Contact book.department@intechopen.com

Numbers displayed above are based on latest data collected.
For more information visit www.intechopen.com

Chapter 35

Theoretical Solution for Tunneling-Induced Stress Field of Subdeep Buried Tunnel

Qinghua Xiao, Jianguo Liu, Shenxiang Lei, Yu Mao, Bo Gao, Meng Wang and Xiangyu Han

Additional information is available at the end of the chapter

http://dx.doi.org/10.5772/66812

Abstract

In the traditional Kirsch solution of stress field induced by tunneling in rock mass, the body force was not taken into consideration, and therefore the Kirsch solution is limited to demonstrate stress redistribution of deep-buried tunnel. In order to consider the effect of body force on the stress redistribution induced by tunneling, a new secondary stress field solution for tunnel between shallow and deep tunnel (called subdeep tunnel) is developed with elastic mechanics and complex function employed. The stress field from theoretical solution is verified by numerical models, and the results showed good agreements with each other. This solution can be the basic theory in the analysis of the stress and field of subdeep tunnel, which have not been valuated through theoretical study yet.

Keywords: subdeep tunnel, stress field, theoretical analysis, complex function, elastic mechanics

1. Introduction

Tunnels are always classified as shallow and deep in tradition, and the classifying standard is the buried depth of tunnel, also known as h_q, which is the limit height that a pressure arch would form in the surrounding rock, and h_q is dependent on the quality of rock mass and tunnel height (Xu et al., 2000). This classification standard is just an empirical approach and is not based on mechanical behavior of rock mass. When tunneling in intact rock mass near the ground surface, the rock mass have partial self-loading capacity which on the other hand is not enough to reach stability for rock mass. And in the presented research, a new type of tunnel classified as subdeep tunnel is described as: primary stress field of tunnel varies along the depth while the redistribution of secondary stress field of tunnel does not reach the ground surface or just have limited influence.

In general, the tunnel support design follows two kinds of strategies based on the tunnel classification of depth, and essentially, the support design strategy is a response to the stress redistribution and rock failure modes. For shallow tunnel, the surround rock has a very limited capacity to form a pressure arch and is very easy to collapse (Yang and Yang, 2008), and therefore the support system are designed to bear the whole weight of loosen zone above the tunnel (Peng and Liu, 2009; Terzaghi, 1943), and the loosen zone is determined by rock properties and tunnel section shapes (Wang et al., 2014). However, in this design approach self-loading capacity of surround rock is not considered in subdeep tunnel, especially in intact rock mass, which would cause a significant waste of materials and always brings uneconomic results. On the other hand, according to the definition of subdeep tunnel, pressure arch which requires a significant burying depth cannot form and thus self-stability cannot be expected, which makes researches on the pressure arch (Li, 2006; Poulsen, 2010; Sansone and Silva, 1998) and support design not suitable for subdeep tunnel.

For a better understanding of mechanical behavior of surround rock for subdeep tunnel, which is the basis for a reasonable support design, a theoretical solution of secondary stress field is put forward with elastic mechanics and complex function adopted. And the derivation process is described in detail as well as the results. The stress field including radial, tangential, and shear stresses are described and discussed. For an intuitive comparison, a numerical model is also built and the results from both theoretical and numerical models are presented, which is a powerful verification for the theoretical solution. Besides, the reasonable depth of subdeep tunnel is suggested by the theoretical results. And this solution for subdeep tunnel can be a very useful theoretical basis for safe and economic tunneling.

2. Theoretical model and primary stresses for subdeep tunnel

2.1. Subdeep tunnel model

In the stress analysis of subdeep tunnel, the following assumptions are made:

- The rock mass is elastic, homogeneous, and intact;
- Only self-weight induced stress field exists in the tunnel site;
- The whole section of the tunnel is excavated in one step; and
- The tunnel is long enough and the model can be treated as planer strain.

As shown in **Figure 1**, a circular tunnel with a radius of a is excavated at depth of h_t. The vertical stress σ_z at the bottom boundary is caused by the self-weight of rock mass and $\sigma_z = 0$ at the ground surface; horizontal stress σ_x varies along z. And this stress field model can be decomposed into two parts, one is the primary stress field as shown in **Figure 1(b)**, and the other is induced by stress-released at tunnel boundary, as shown in **Figure 1(c)**.

The primary stress field in **Figure 1(b)** can be described as follows according to Heim's hypothesis (Fegert, 2013) and Gold Nick's hypothesis (Dessler, 1982):

http://dx.doi.org/10.5772/66812

$$\begin{cases} \sigma_z = \gamma(h_t - z) \\ \sigma_x = k_0\sigma_z = k_0\gamma(h_t - z) \\ \tau_{xz} = 0 \end{cases} \tag{1}$$

where z is the coordinate from tunnel center; k_0 is the lateral stress coefficient; h_t is the depth from the tunnel center to ground; and $k_0 = \frac{\nu}{1-\nu}$.

2.2. Analysis of the stress to release at tunnel boundary

The stress in polar coordinates in **Figure 1** can be converted from Eq. (1) in rectangular coordinates as follows:

$$\begin{cases} \sigma_r = \sigma_x \cos^2\theta + \sigma_z \sin^2\theta + \tau_{xz} \sin 2\theta = \dfrac{\sigma_z + \sigma_x}{2} - \dfrac{\sigma_z - \sigma_x}{2} \cos 2\theta + \tau_{xz} \sin 2\theta \\ \sigma_\theta = \sigma_x \sin^2\theta + \sigma_z \cos^2\theta - \tau_{xz} \sin 2\theta = \dfrac{\sigma_z + \sigma_x}{2} + \dfrac{\sigma_z - \sigma_x}{2} \cos 2\theta - \tau_{xz} \sin 2\theta \\ \tau_{r\theta} = \dfrac{\sigma_z - \sigma_x}{2} \sin 2\theta + \tau_{xz} \cos 2\theta \end{cases} \tag{2}$$

Where σ_r = radial stress, σ_θ= tangential stress, and $\tau_{r\theta}$= shear stress.

By submitting Eq. (1) into Eq. (2), the primary stress field can be expressed as:

$$\begin{cases} \sigma_r = \dfrac{1 + k_0}{2}\gamma(h_t - z) - \dfrac{1 - k_0}{2}\gamma(h_t - z)\cos 2\theta \\ \sigma_\theta = \dfrac{1 + k_0}{2}\gamma(h_t - z) + \dfrac{1 - k_0}{2}\gamma(h_t - z)\cos 2\theta \\ \tau_{r\theta} = \dfrac{1 - k_0}{2}\gamma(h_t - z)\sin 2\theta \end{cases} \tag{3}$$

where $z = r\sin\theta$.

When $r = a$, which means at the tunnel boundary:

$$\begin{cases} \sigma^0_{ra} = \dfrac{1 + k_0}{2}\gamma(h_t - a\sin\theta) - \dfrac{1 - k_0}{2}\gamma(h_t - a\sin\theta)\cos 2\theta \\ \sigma^0_{\theta a} = \dfrac{1 + k_0}{2}\gamma(h_t - a\sin\theta) + \dfrac{1 - k_0}{2}\gamma(h_t - a\sin\theta)\cos 2\theta \\ \tau^0_{r\theta a} = \dfrac{1 - k_0}{2}\gamma(h_t - a\sin\theta)\sin 2\theta \end{cases} \tag{4}$$

Then, Eq. (4) is the stress to release in the following steps shown in **Figure 1**.

2.3. Complex function for elastic mechanics

With complex function, stress components in **Figure 1** in polar coordinate can be expressed as

$$z : \begin{cases} \sigma_\theta + \sigma_r = 4\mathrm{Re}\chi'_1(z) \\ \sigma_\theta - \sigma_r + 2\mathrm{i}\tau_{r\theta} = 2[\overline{z}\chi''_1(z) + \psi'_1(z)]\mathrm{e}^{2\mathrm{i}\lambda} \end{cases} \tag{5}$$

where Re is the real part of complex function, $\overline{z}$ is the conjugate expression of z, $\chi_1(z)$ and $\psi_1(z)$

are complex potential function, $\chi_1^{'}(z)$ and $\chi_1^{''}(z)$ are the first and second derivatives of $\chi_1(z)$, respectively, and $\psi_1^{'}(z)$ is the first derivative of $\psi_1(z)$.

2.4. Stress release

Similar to the solving process of an infinite plate with a hole (Wang, 2008), as the stress field approximates to zero, the solving process are described as follows:

1. Submitting Eq. (4) into the Fourier coefficient equations;
2. Through the obtained equations, solving the constant coefficients; and
3. As the problem has been assumed to be a planar strain work, which means $k_0 = \frac{\nu}{1-\nu} = \nu^{'}$, the following equations can be obtained based on steps (1) and (2):

$$\begin{cases} \chi^{'}{}_1(z) = \dfrac{a_1}{z} + \dfrac{a_2}{z^2} + \dfrac{a_3}{z^3} = \dfrac{(1+\nu^{'})\gamma a^2}{8}\dfrac{\mathrm{i}}{z} + \dfrac{(1-k_0)\gamma h_t a^2}{2}\dfrac{1}{z^2} - \dfrac{(1-k_0)\gamma a^4}{4}\dfrac{\mathrm{i}}{z^3} \\ \overline{\chi^{'}{}_1(z)} = \dfrac{\overline{a}_1}{\overline{z}} + \dfrac{\overline{a}_2}{\overline{z}^2} + \dfrac{\overline{a}_3}{\overline{z}^3} = -\dfrac{(1+\nu^{'})\gamma a^2}{8}\mathrm{i}\overline{z} + \dfrac{(1-k_0)\gamma h_t a^2}{2}\dfrac{1}{\overline{z}^2} + \dfrac{(1-k_0)\gamma a^4}{4}\dfrac{\mathrm{i}}{\overline{z}^3} \\ \chi^{''}{}_1(z) = \dfrac{-a_1}{z^2} + \dfrac{-2a_2}{z^3} + \dfrac{-3a_3}{z^4} = -\dfrac{(1+\nu^{'})\gamma a^2}{8}\dfrac{\mathrm{i}}{z^2} - \dfrac{2(1-k_0)\gamma h_t a^2}{2}\dfrac{1}{z^3} + \dfrac{3(1-k_0)\gamma a^4}{4}\dfrac{\mathrm{i}}{z^4} \\ \psi^{'}{}_1(z) = \dfrac{b_1}{z} + \dfrac{b_2}{z^2} + \dfrac{b_3}{z^3} + \dfrac{b_4}{z^4} + \dfrac{b_5}{z^5} = \dfrac{(3-\nu^{'})\gamma a^2}{8}\dfrac{\mathrm{i}}{z} + \dfrac{(1+k_0)\gamma h_t a^2}{2}\dfrac{1}{z^2} + \dfrac{(\nu^{'}-k_0)\gamma a^4}{4}\dfrac{\mathrm{i}}{z^3} \\ \qquad + \dfrac{3(1-k_0)\gamma h_t a^4}{2}\dfrac{1}{z^4} - (1-k_0)\gamma a^6\dfrac{\mathrm{i}}{z^5} \\ \chi_1(z) = \dfrac{(1+\nu^{'})\gamma a^2}{8}\mathrm{i}\ln z - \dfrac{(1-k_0)\gamma h_t a^2}{2}\dfrac{1}{z} + \dfrac{(1-k_0)\gamma a^4}{8}\dfrac{\mathrm{i}}{z^2} + c_1 \\ \psi_1(z) = \dfrac{(3-\nu^{'})\gamma a^2}{8}\mathrm{i}\ln z - \dfrac{(1+k_0)\gamma h_t a^2}{2}\dfrac{1}{z} - \dfrac{(\nu^{'}-k_0)\gamma a^4}{8}\dfrac{\mathrm{i}}{z^2} - \dfrac{(1-k_0)\gamma h_t a^4}{2}\dfrac{1}{z^3} + \dfrac{(1-k_0)\gamma a^6}{4}\dfrac{\mathrm{i}}{z^4} + c_2 \\ \overline{\psi_1(z)} = \dfrac{(3-\nu^{'})\gamma a^2}{8}\mathrm{i}\ln\overline{z} - \dfrac{(1+k_0)\gamma h_t a^2}{2}1\overline{z} + \dfrac{(\nu^{'}-k_0)\gamma a^4}{8}\dfrac{\mathrm{i}}{\overline{z}^2} - \dfrac{(1-k_0)\gamma h_t a^4}{2}\dfrac{1}{\overline{z}^3} - \dfrac{(1-k_0)\gamma a^6}{4}\dfrac{\mathrm{i}}{\overline{z}^4} + \overline{c}_2 \end{cases} \tag{6}$$

By submitting Eq. (6) into Eq. (5), the relation between stress components can be expressed by:

$$\begin{cases} \sigma_\theta + \sigma_r = 2\mathrm{Re}\left(\dfrac{(1+\nu^{'})\gamma a^2}{4}\dfrac{\mathrm{i}}{z} + (1-k_0)\gamma h_t a^2\dfrac{1}{z^2} - \dfrac{(1-k_0)\gamma a^4}{2}\dfrac{\mathrm{i}}{z^3}\right) \\ \sigma_\theta - \sigma_r + 2\mathrm{i}\tau_{r\theta} = 2[\overline{z}\chi^{''}{}_1(z) + \psi^{'}{}_1(z)]\mathrm{e}^{2\mathrm{i}\theta} \\ = 2\left[-\dfrac{(1+\nu^{'})\gamma a^2}{8}\dfrac{\overline{z}\mathrm{i}}{z^2} - \dfrac{2(1-k_0)\gamma h_t a^2}{2}\dfrac{\overline{z}}{z^3} + \dfrac{3(1-k_0)\gamma a^4}{4}\dfrac{\overline{z}\mathrm{i}}{z^4} + \dfrac{(3-\nu^{'})\gamma a^2}{8}\dfrac{\mathrm{i}}{z}\right. \\ \quad \left. + \dfrac{(1+k_0)\gamma h_t a^2}{2}\dfrac{1}{z^2} + \dfrac{(\nu^{'}-k_0)\gamma a^4}{4}\dfrac{\mathrm{i}}{z^3} + \dfrac{3(1-k_0)\gamma h_t a^4}{2}\dfrac{1}{z^4} - (1-k_0)\gamma a^6\dfrac{\mathrm{i}}{z^5}\right]\mathrm{e}^{2\mathrm{i}\theta} \end{cases} \tag{7}$$

where z, which is a complex valuable, can be expressed as:

http://dx.doi.org/10.5772/66812

$$\begin{cases} \dfrac{\mathrm{i}}{z}=\dfrac{\mathrm{i}}{r\mathrm{e}^{\mathrm{i}\theta}}=\dfrac{\mathrm{i}\mathrm{e}^{-\mathrm{i}\theta}}{r}=\dfrac{\sin\theta+\mathrm{i}\cos\theta}{r} \\ \dfrac{1}{z^2}=\dfrac{1}{r^2\mathrm{e}^{\mathrm{i}2\theta}}=\dfrac{\mathrm{e}^{-\mathrm{i}2\theta}}{r^2}=\dfrac{\cos 2\theta-\mathrm{i}\sin 2\theta}{r^2} \\ \dfrac{\mathrm{i}}{z^3}=\dfrac{\mathrm{i}}{r^3\mathrm{e}^{\mathrm{i}3\theta}}=\dfrac{\mathrm{i}\mathrm{e}^{-\mathrm{i}3\theta}}{r^3}=\dfrac{\sin 3\theta+\mathrm{i}\cos 3\theta}{r^3} \end{cases} \tag{8}$$

By submitting Eq. (8) into the Eq. (7), a more simple relation between stress components are obtained, and by decomposing the imaginary part in the obtained equations, the subsidiary stress induced by the stress release process in **Figure 1** is obtained. The obtained subsidiary stress is based on the infinite plate assumption, and it is an approximate value. For a more accurate solution, the subsidiary stress at ground surface should be released again, which is a very complicated process. By solving the obtained subsidiary stress components with Eq. (3), the stress field solution for subdeep tunnel can be expressed as:

$$\begin{cases} \sigma_r=\dfrac{1+k_0}{2}\gamma(h_t-r\sin\theta)-\dfrac{1-k_0}{2}\gamma(h_t-r\sin\theta)\cos 2\theta+\gamma\left\{-\dfrac{(1+k_0)h_t a^2}{2r^2}\right. \\ \quad\left.+\left[\dfrac{(3+\nu')a^2}{4r}+\dfrac{(\nu'-k_0)a^4}{4r^3}\right]\sin\theta+(1-k_0)h_t\left(\dfrac{2a^2}{r^2}-\dfrac{3a^4}{2r^4}\right)\cos 2\theta-(1-k_0)a\left(\dfrac{5a^3}{4r^3}-\dfrac{a^5}{r^5}\right)\sin 3\theta\right\} \\ \sigma_\theta=\dfrac{1+k_0}{2}\gamma(h_t-r\sin\theta)+\dfrac{1-k_0}{2}\gamma(h_t-r\sin\theta)\cos 2\theta+\gamma\left\{\dfrac{(1+k_0)h_t a^2}{2r^2}\right. \\ \left.-\left[\dfrac{(1-\nu')a^2}{4r}-\dfrac{(\nu'-k_0)a^4}{4r^3}\right]\sin\theta+(1-k_0)h_t\dfrac{3a^4}{2r^4}\cos 2\theta+(1-k_0)a\left(\dfrac{a^3}{4r^3}-\dfrac{a^5}{r^5}\right)\sin 3\theta\right\} \\ \tau_{r\theta}=\dfrac{1-k_0}{2}\gamma(h_t-r\sin\theta)\sin 2\theta \\ +\gamma\left[\dfrac{(1-\nu')a^2}{4r}+\dfrac{(\nu'-k_0)a^4}{4r^3}\right]\cos\theta+(1-k_0)h_t\left(\dfrac{a^2}{r^2}-\dfrac{3a^4}{2r^4}\right)\sin 2\theta+(1-k_0)a\left(\dfrac{3a^3}{4r^3}-\dfrac{a^5}{r^5}\right)\cos 3\theta\} \end{cases} \tag{9}$$

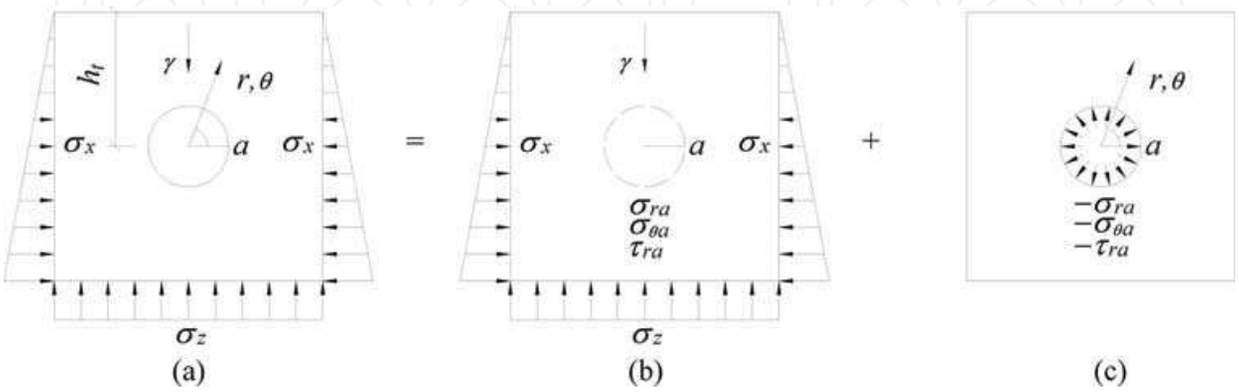

Figure 1. Mechanical model and decomposition of the secondary stress field of subdeep tunnel. (a) Secondary stress field. (b) Primary stress field. (c) Stress released.

3. Distribution of secondary stress field solution for subdeep tunnel

The secondary stress field of subdeep tunnel calculated from Eq. (9), and the v, and h_t are set at 0.3 and 6a, respectively. The results are shown in **Figure 2**.

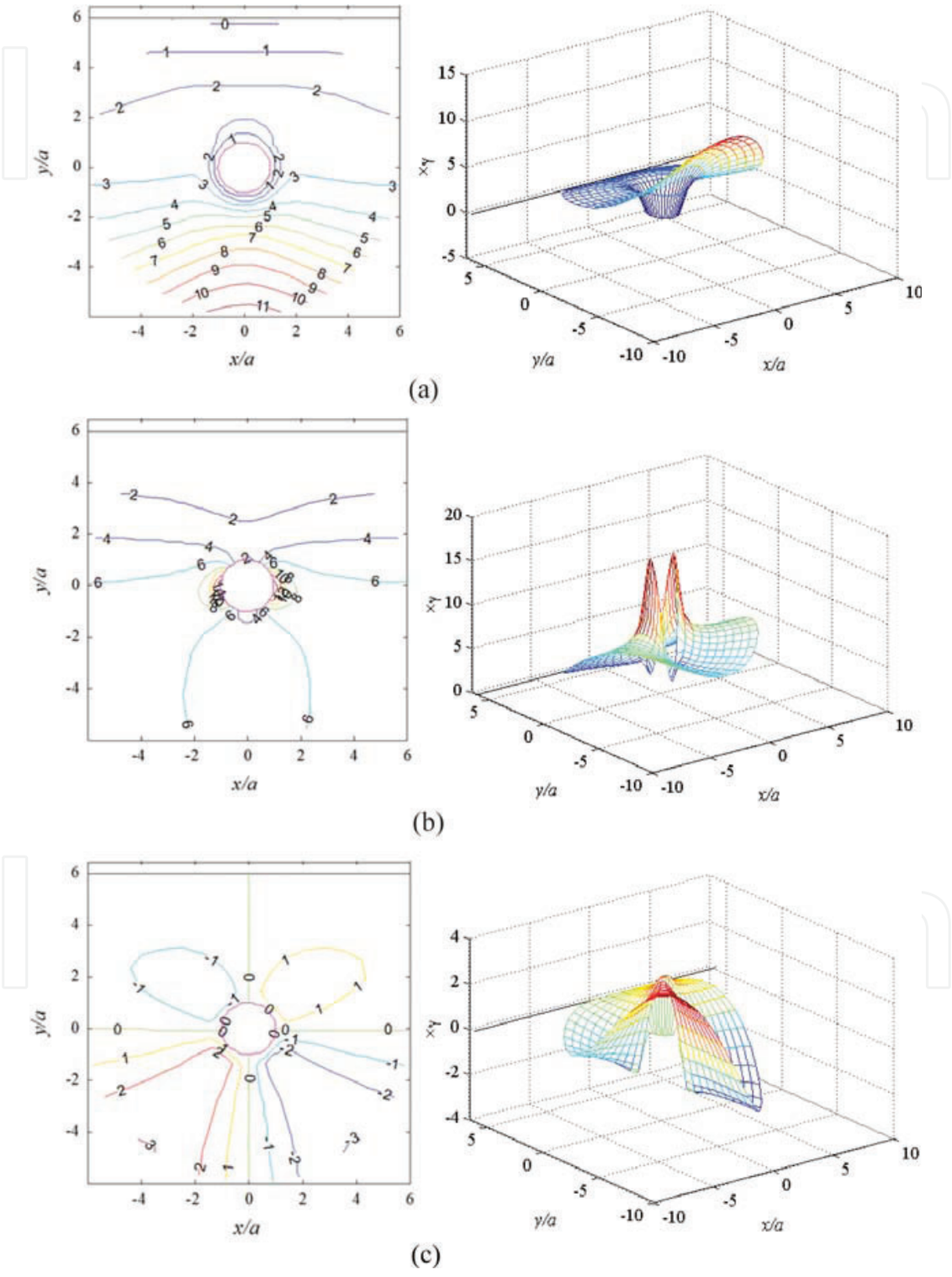

Figure 2. Second stress distribution in subdeep tunnels. (a) Distribution of σ_r. (b) Distribution of σ_θ. (c) Distribution of $\tau_{r\theta}$.

http://dx.doi.org/10.5772/66812

Stress distribution along r different directions in polar coordinate are also illustrated in **Figure 3** in a normalized form.

From **Figures 2** and **3**, the distributions of secondary stress field induced by tunneling for subdeep tunnel are different from the deep-buried tunnels, which has the following characteristics of its own:

1. The distribution of secondary subdeep tunnel just shows axial symmetry, not like the deep-buried tunnel, whose stress field shows bidirectional symmetry. This difference is caused by the variation of σ_z along z in the primary field.
2. The tangential stress near the tunnel boundary shows significant concentration at the side wall of the tunnel, to which close attention should be paid.

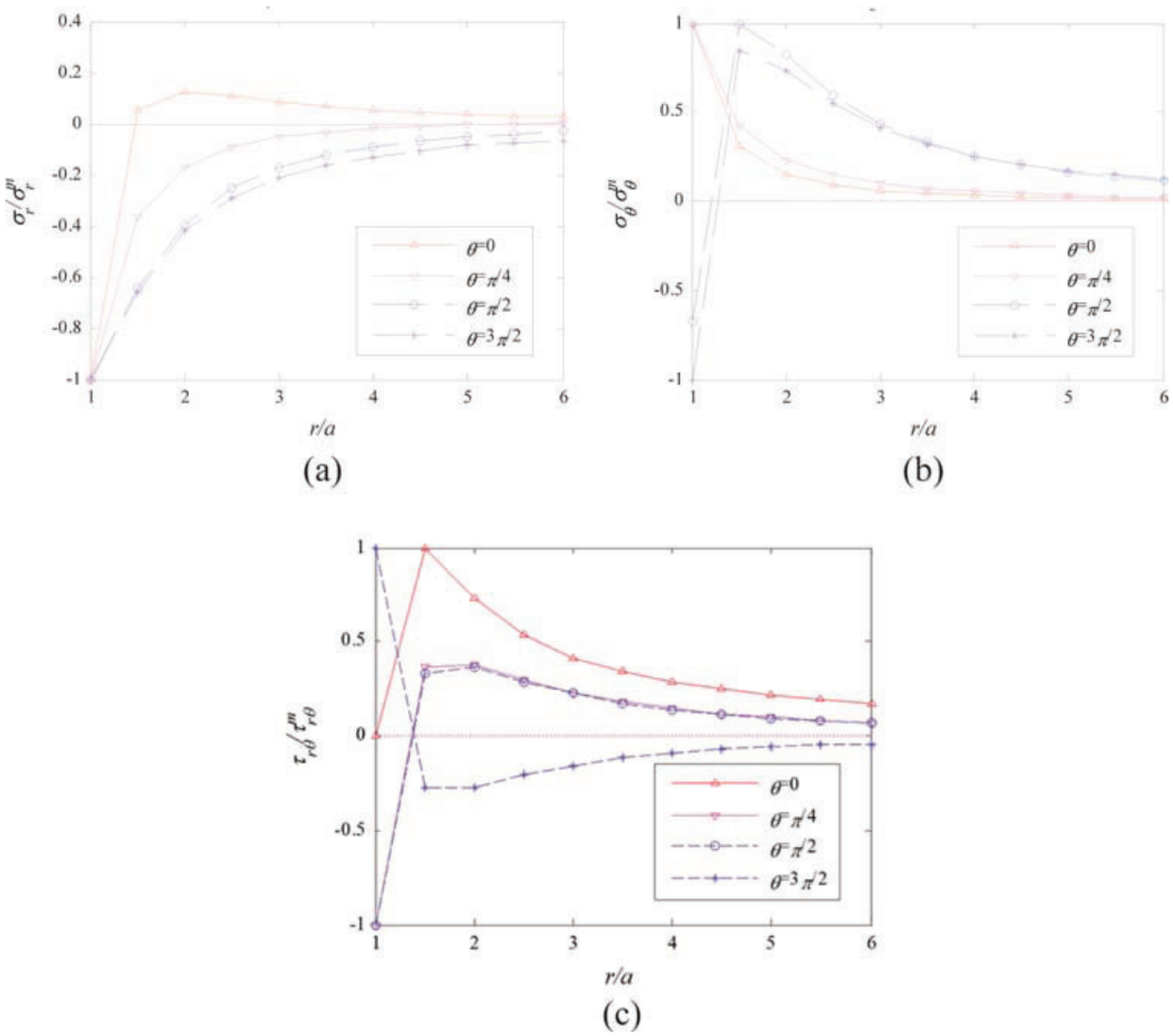

Figure 3. Stress distribution along r different directions. (a) Distribution of σ_r along r. (b) Distribution of σ_θ along r. (c) Distribution of $\tau_{r\theta}$ along r.

3. **Figure 3** shows the variation of stress induced by tunneling along polar radius, and it is quite clear that, the stresses are approximate to 0, which proves the simplification of zero stress boundary to be reasonable and correct. Besides, subdeep tunnel can be determined as tunnels buried at depth of more than 2.5 D (D is the diameter of tunnel), and less than the depth of deep tunnel.

From the stress analysis, secondary stress field for subdeep tunnel is demonstrated and the limit depth to distinguish shallow tunnel and subdeep tunnel is obtained, which can be the guideline for tunnel support in a more reasonable, economic, and safer way.

4. Numerical solution and its comparison with theoretical results

To verify the theoretical solution, a numerical model is developed. The parameters for theoretical and numerical simulation are shown in **Table 1**. And a numerical model is developed in Flac3D as shown in **Figure 4**.

Theoretical solution of horizontal stresses (σ_{xx}) of surrounding rock in subdeep tunnel is shown in **Figure 5(a)** in a rectangular coordinate system, and its numerical result is shown in **Figure 5(b)**.

Theoretical solution of vertical stresses (σ_{zz}) of surrounding rock in subdeep tunnel is shown in **Figure 6(a)**, and the numerical result is shown in **Figure 6(b)**.

Theoretical solution of shear stresses (τ_{xz}) of surrounding rock in subdeep tunnel is shown in **Figure 7(a)**, and its numerical result is shown in **Figure 7(b)**.

Contours of horizontal and vertical stress field from theoretical and numerical solution show good agreement with each other as shown in **Figures 5** and **6**, which proves the theoretical analysis reasonable and correct. On the other hand, shear stress from theoretical and numerical solution shows difference to some extent. In **Figure 7**, shear stress, from numerical solution, has a much smaller distribution area than that from numerical model, a probable explanation is that, the media in theoretical model is elastic while that in numerical model is elastic-plastic, and stress concentration near the tunnel boundary may redistribute after rock failure, leading to a smoother distribution of shear stress in numerical model.

Parameters of theoretical solution				**Parameters of numerical simulation**			
Item	**Symbol**	**Value**	**Unit**	**Item**	**Symbol**	**Value**	**Unit**
Tunnel's radius	a	3	m	Tunnel's radius	a	3	m
Depth of tunnel center	h_t	6 a	m	Depth of tunnel	d	15	m
Volume weight	γ	2.10E+04	N/m^3	Density	ρ	2.10E+03	kg/m^3
Elasticity modulus	E	9.00E+07	Pa	Bulk modulus	K	7.50E+07	Pa
Poisson's ratio	ν	0.30	-	Shear modulus	G	3.46E+07	Pa

Table 1. Parameters for theoretical and numerical simulation.

http://dx.doi.org/10.5772/66812

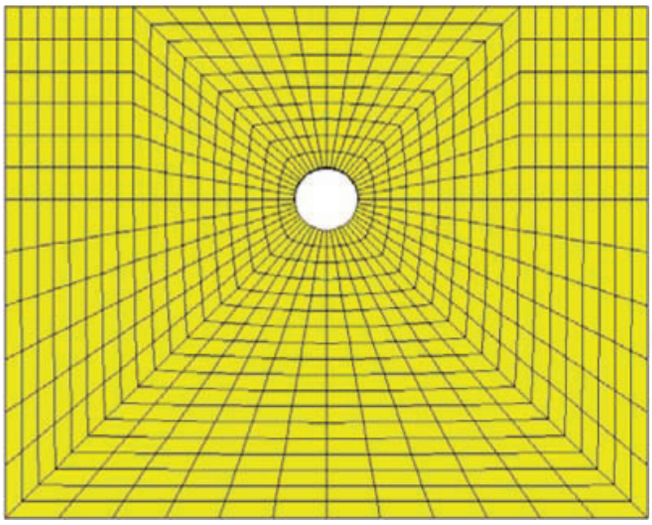

Figure 4. Numerical model of subdeep tunnels.

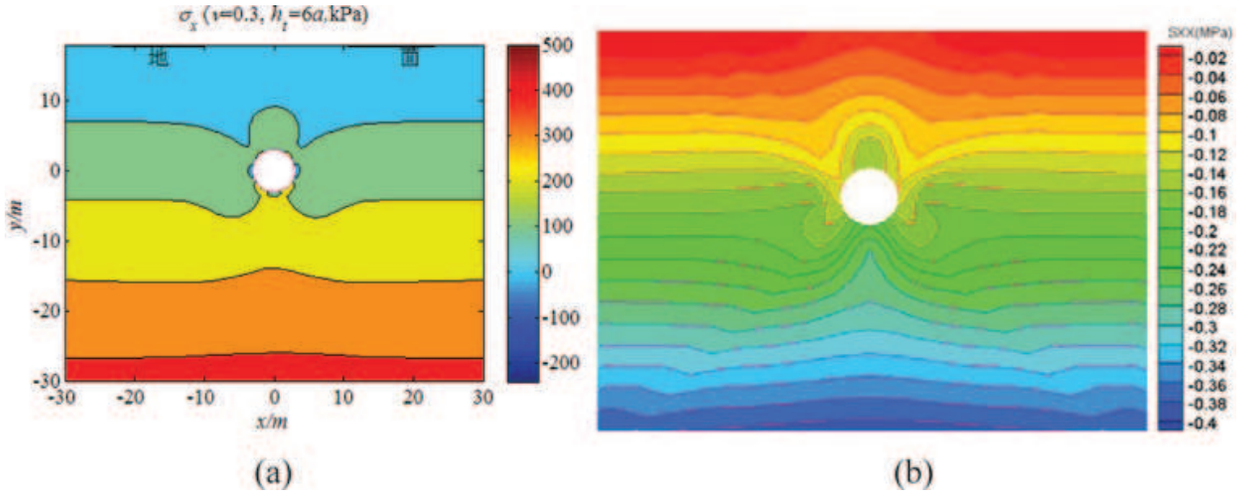

Figure 5. Theoretical and numerical solution of horizontal stress. (a) Theoretical solution. (b) Numerical solution.

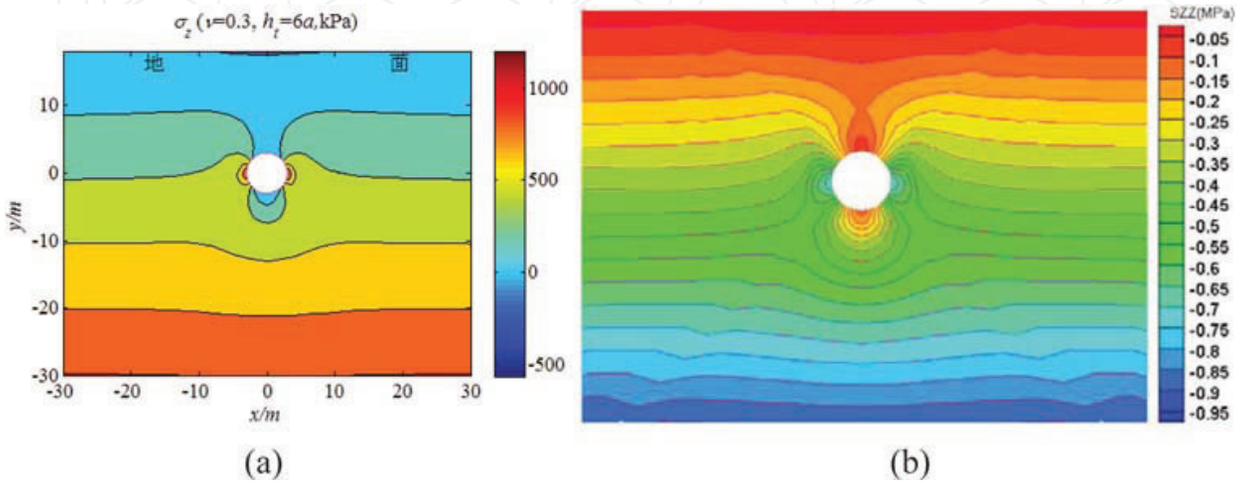

Figure 6. Theoretical solutions and numerical value of vertical stress. (a) Theoretical solution. (b) Numerical solution.

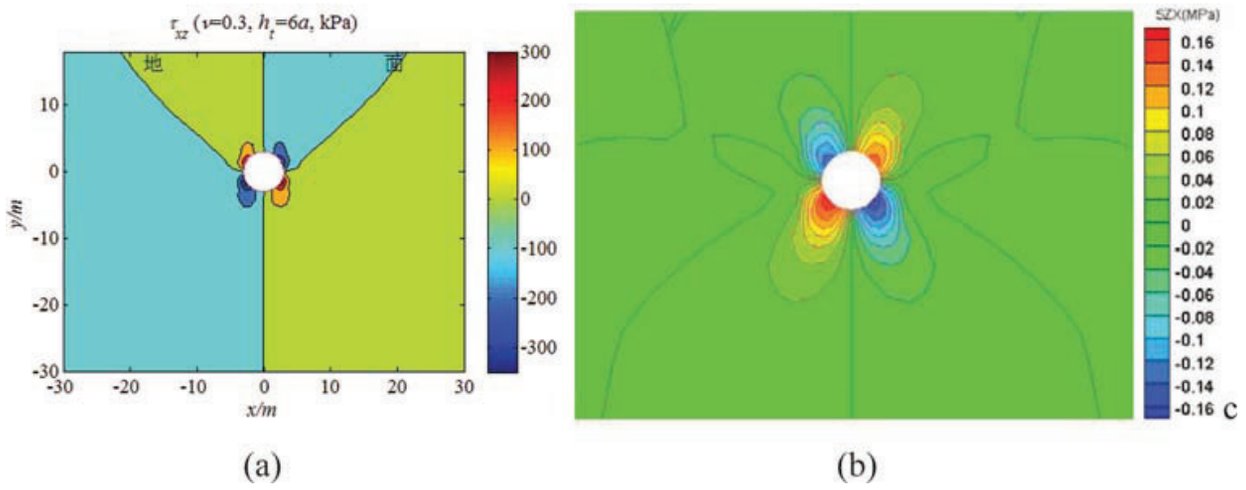

Figure 7. Theoretical and numerical solution of shear stress. (a) Theoretical solution. (b) Numerical solution.

5. Conclusions

In the presented research, the stress field for tunnel buried at depth between deep tunnel and shallow tunnel is analyzed with elastic mechanics and complex function, and conclusions can be drawn as:

1. The subdeep tunnel is proposed and through theoretical analysis, and stress fields show that essential difference exists between the mechanical behavior of deep tunnel and subdeep tunnel, and the depth to distinguish shallow tunnel and subdeep tunnel is suggested as 2.5 times of the tunnel diameter.
2. By numerical analysis, the theoretical solution is proved to be reasonable and with high accuracy. And this theoretical solution can be a very good guideline for the support design for subdeep tunnel with economy and safety.
3. This theoretical solution also has its limitations, and if used for deep tunnels, the vertical stress in rock would be incorrect totally. Besides, this solution is not suitable for tunnels buried in depth less than 2.5 D, which does not satisfy the boundary stress condition.
4. Through the comparison of theoretical analysis and numerical model, the theoretical results are proved to be effective in the determination of subdeep tunnel, which can be very helpful in the design of subtunnel support for economy and safety purpose.

Author details

Qinghua Xiao[1]*, Jianguo Liu[1], Shenxiang Lei[1,2], Yu Mao[1], Bo Gao[1], Meng Wang[1] and Xiangyu Han[1]

*Address all correspondence to: xqhbp@home.swjtu.edu.cn

1 School of Civil Engineering, Southwest Jiaotong University, Chengdu, China

2 China Railway 20th Bureau, Xi'an, China

http://dx.doi.org/10.5772/66812

References

A. J. Dessler. Gold's hypothesis and the energetics of the Jovian magnetosphere. Cosmology & Astrophysics Essays in Honor of Thomas Gold Ithaca, 137–143,1982 http://adsabs.harvard.edu/abs/1982coas.conf.137D.

M. D. Fegert. The insufficiency of S. Mark Heim's more pluralistic hypothesis. Theology Today 69, 497–510, 2013.

C. C. Li. Rock support design based on the concept of pressure arch. International Journal of Rock Mechanics & Mining Sciences 43, 1083–1090, 2006.

L. M. Peng, X. B. Liu. Tunneling Engineering. Central South University Press, Changsha, 2009.

B. A. Poulsen. Coal pillar load calculation by pressure arch theory and near field extraction ratio. International Journal of Rock Mechanics & Mining Sciences 47, 1158–1165, 2010.

E. C. Sansone, L. A. A. D. Silva. Numerical modeling of the pressure arch in underground mines. International Journal of Rock Mechanics & Mining Sciences 35, 436, 1989.

K. Terzaghi. Theoretical Soil Mechanics. John Wiley & Sons, New York, 1943.

G. Wang. Elastic Mechanics. China Railway Publishing House, Beijing, 2008.

Z. Wang, C. Qiao, C. Song, J. Xu. Upper bound limit analysis of support pressures of shallow tunnels in layered jointed rock strata. Tunnelling and Underground Space Technology 43, 171–183, 2014.

Z. Xu., R. Huang, S. Wang. Tunnel classifying in light of depth (i.e. thickness of overburden). The Chinese Journal of Geological Hazard and Control 11, 5–10, 2000.

F. Yang, J. Yang.. Limit analysis method for determination of earth pressure on shallow tunnel. Engineering Mechanics 25, 6, 2008.

IntechOpen